ADVANCED FUNCTIONAL MATERIALS
www.afm-journal.de

Mussel-Inspired Contact-Active Antibacterial Hydrogel with High Cell Affinity, Toughness, and Recoverability

*Donglin Gan, Tong Xu, Wensi Xing, Xiang Ge, Liming Fang, Kefeng Wang, Fuzeng Ren, and Xiong Lu**

Antibacterial hydrogel has received extensive attention in soft tissue repair, especially preventing infections those associated with impaired wound healing. However, it is challenging in developing an inherent antibacterial hydrogel integrating with excellent cell affinity and superior mechanical properties. Inspired by the mussel adhesion chemistry, a contact-active antibacterial hydrogel is proposed by copolymerization of methacrylamide dopamine (MADA) and 2-(dimethylamino)ethyl methacrylate and forming an interpenetrated network with quaternized chitosan. The reactive catechol groups of MADA endow the hydrogel with contact intensified bactericidal activity, because it increases the exposure of bacterial cells to the positively charged groups of the hydrogel and strengthens the bactericidal effect. MADA also maintains the good adhesion of fibroblasts to the hydrogel. Moreover, the hybrid chemical and physical cross-links inner the hydrogel network makes the hydrogel strong and tough with good recoverability. In vitro and in vivo tests demonstrate that this tough and contact-active antibacterial hydrogel is a promising material to fulfill the dual functions of promoting tissue regeneration and preventing bacterial infection for wound-healing applications.

1. Introduction

Wound infection generally causes prolonged wound healing and implantation failure and results in other serious problems, even mortality. Recently developed antibacterial hydrogels offer new possibilities for fighting bacterial infectious diseases because hydrogel has high water swell-ability, high oxygen permeability, and structure diversity.[1] Antibacterial hydrogels generally immobilize antibiotics to prevent bacterial infection; however, the excessive use of antibiotics leads to bacterial resistance. Other antibacterial hydrogels incorporate bactericidal agents into the hydrogel network, including silver nanoparticles, which might cause cytotoxicity. Therefore, the biocompatibility of bactericidal agents contained hydrogels is a major concern. Employing inherent antibacterial materials, including cationic polymers, may be a feasible solution to develop long-lasting inherent antimicrobial hydrogels. Synthetic quaternary ammonium polymers are forms of cationic polymers that exhibit good antimicrobial ability because of the presence of a large number of cations on the polymer chain. However, synthetic quaternary ammonium polymers display poor cell and tissue affinities. Biocompatible natural polymers, including chitosan (CS) and quaternized chitosan (QCS), are also widely used antibacterial biopolymers, because of their high density of positively charged groups, which have been prepared as hydrogels[2] and scaffolds[3] to apply as antibacterial treatments. It should be noted that the previously reported antibacterial hydrogels based on quaternary ammonium polymers generally possess low antibacterial activity under the in vivo environment.[4] Therefore, it is urgent to develop hydrogels with high antibacterial activity and long-term efficacy while being free of toxic agents and antibiotics.

In addition to antibacterial properties, excellent mechanical properties, including high toughness, good flexibility, and

D. Gan, T. Xu, W. Xing, Prof. X. Lu
Key Lab of Advanced Technologies of Materials
Ministry of Education
School of Materials Science and Engineering
Southwest Jiaotong University
Chengdu, Sichuan 610031, China
E-mail: luxiong_2004@163.com
Dr. X. Ge
Key Laboratory of Mechanism Theory and Equipment Design
of the Ministry of Education
School of Mechanical Engineering
Tianjin University
Tianjin 300354, China
The ORCID identification number(s) for the author(s) of this article can be found under https://doi.org/10.1002/adfm.201805964.
Dr. L. M. Fang
Department of Polymer Science and Engineering
School of Materials Science and Engineering
South China University of Technology
Guangzhou 510541, China
Dr. K. F. Wang
National Engineering Research Center for Biomaterials
Sichuan University
Chengdu 610064, China
Dr. F. Z. Ren
Department of Materials Science and Engineering
Southern University of Science and Technology
Shenzhen, Guangdong 518055, China

DOI: 10.1002/adfm.201805964

recoverability, are the essential requirement of hydrogels for soft tissue repair. Recently, tough hydrogels, including interpenetrating network hydrogel,[5] double-network hydrogel,[6] and nanocomposite hydrogel,[7] have been designed for tissue regeneration, because they have good mechanical properties matching soft tissue. Polyampholyte hydrogels are one of the most commonly encountered form of tough hydrogel, which are synthesized with positively and negatively charged units. These oppositely charged groups form a high density of electrostatic interaction within the hydrogel network, and therefore, endow the polyampholyte hydrogels with good mechanical properties. King et al.[8] produced a tough composite hydrogel, consisting of a polyampholyte hydrogel and a glass fiber woven fabric, which exhibited high toughness, tear strength, and tensile modulus. Sun and co-workers[9] described a series of physical hydrogels composed of polyampholytes with high toughness and viscoelasticity. You et al.[10] developed a series of QCS/poly (acrylic acid) (PAA) hydrogels with high mechanical strength and shape-memory behavior in deionized water and other solutions. However, most of these tough hydrogels are cell repellent, thereby limiting their applications in biomedical engineering.

Polydopamine (PDA) shed new light on preparing cell affinitive and adhesive materials, because it shares similar molecular structures with adhesive protein of mussels. The catechol groups of PDA can undergo hydrogen bonding, electrostatic interaction, and π–π interaction with various surfaces, which endows materials with good cell/tissue adhesive properties. Han et al.[11] developed a form of mussel-inspired hydrogel, which displayed stretchable, self-adhesive, and self-healable abilities, and can be used for sensor and cartilage regeneration. Shao et al.[12] prepared a mussel-inspired cellulose composite hydrogel, which exhibited high toughness and strain sensitivity. In addition, PDA could be used to prepare cell-friendly antibacterial hydrogels. For example, Fullenkamp et al.[13] reported a mussel-inspired silver-releasing antibacterial hydrogel with low cell toxicity and good bactericidal ability. Campo and co-workers[14] reported that Cl-dopamine-modified hydrogels have a potential to prevent biofilm formation. Sileika et al.[15] deposited PDA functionalized silver nanoparticles into a PDA-based hydrogel layer, which improved antimicrobial performance of substrate materials. In summary, dopamine and its derivatives incorporation is expected to endow hydrogels with various prominent properties, including cell affinity, adhesiveness, and high toughness.

In this study, we describe a mussel-inspired contact-active antibacterial polyampholyte hydrogel with high toughness and resilience and remarkable cell/tissue affinity. To synthesize the contact-active antibacterial hydrogel, chitosan (CS) was first quaternized using glycidyltrimethylammonium chloride (**Figure 1**a), and dopamine was also modified using methacrylic anhydride (Figure 1b). Then, AA-co-MADA-co-DMAEMA (AMD) terpolymer were generated by UV-polymerization of methacrylamide dopamine (MADA), acrylic acid (AA), and 2-(dimethylamino)ethyl methacrylate (DMAEMA), and positively charged QCS was interpenetrated into the terpolymer network to form the antibacterial hydrogel AMD-QCS by a one-pot method (Figure 1c). The hydrogels have the following prominent advantages. First, unlike previously reported antibiotics or nanoparticle incorporated antibacterial hydrogels, the current hydrogel exhibited inherent contact-active antibacterial activities. MADA favors bacterial cell contact with the hydrogel surface when the bacterial cell comes close to the hydrogel, and then the bacterial cells are killed by the DMAEMA and QCS. Second, the hydrogel exhibit both high toughness and good recoverability. The toughness is as high as 9168 J m^{-2}, which is because both chemical and physical cross-linking were present in the hydrogel network. The AMD terpolymer was chemically cross-linked using poly(ethylene glycol) diacrylate (PEGDA) as the cross-linker, while QCS was incorporated into the hydrogel to form physical cross-linking with the AMD terpolymer. The copolymerization of MADA further tune the density of physical cross-linking. The synergistic effect of chemical and physical cross-linking endows the hydrogel with high toughness and good recoverability. Finally, unlike previous tough or antibacterial hydrogels that were generally cell repellent, the current hydrogel exhibited high cell and tissue affinity due to the reactive catechol groups of MADA. In short, this study proposed a contact-active antibacterial hydrogel with a new bactericidal mechanism, which is likely suitable to accelerate soft tissue repair and protect wound from bacterial infection. Abbreviations list of various materials is listed in Table SI in the Supporting Information.

2. Results

2.1. The Mechanical Properties of the Hydrogels

The AMD-QCS hydrogel exhibited a good mechanical performance, particularly in recoverability. This hydrogel in a cylindrical form withstood a high compression strain of 85% without breaking (**Figure 2**a). After removing the compression force, the hydrogel immediately recovered its original shape. Additionally, the hydrogel recovered its initial length after it was stretched to a tensile strain of 200% (Figure 2b). By contrast, the AD-QCS hydrogel failed to recover after compression or tensile strain. These results revealed that the copolymerization of MADA in the hydrogel was critical to endow the hydrogel with good recoverability. The AMD-QCS hydrogel also exhibited good flexibility and toughness. After knotting the AMD-QCS hydrogel to produce a noodle-like shape (diameter = 5 mm), the hydrogel was able to sustain a large load of up to 500 g (Figure 2c). The hydrogel was sufficiently tough so as not to be readily cut with a blade (Figure 2d). Typical compressive stress–strain curves of the various hydrogels are presented in Figure 2e. Both MADA and QCS addition greatly increased the compressive strength (1.3 MPa) (Figure S4, Supporting Information) and compressive modulus (15.3 MPa) (Figure 2f) of the hydrogels. The loading–unloading compressive test of the AMD-QCS hydrogel showed that this hydrogel was able to recover its original state after compressive force was released (Figure 2g). Typical tensile stress–strain curves of the four hydrogels in uniaxial tensile tests are presented in Figure 2h. The AMD-QCS hydrogel displayed a maximum tensile strength of 1.1 MPa, higher than that of AD-QCS (0.7 MPa), and in clear contrast to that of the AMD (0.2 MPa) and AD hydrogels (0.2 MPa). The tensile modulus of the AMD-QCS hydrogel was ≈1.5 MPa, much higher than that of the other three hydrogels (Figure 2i). The fracture energy increased after the addition of

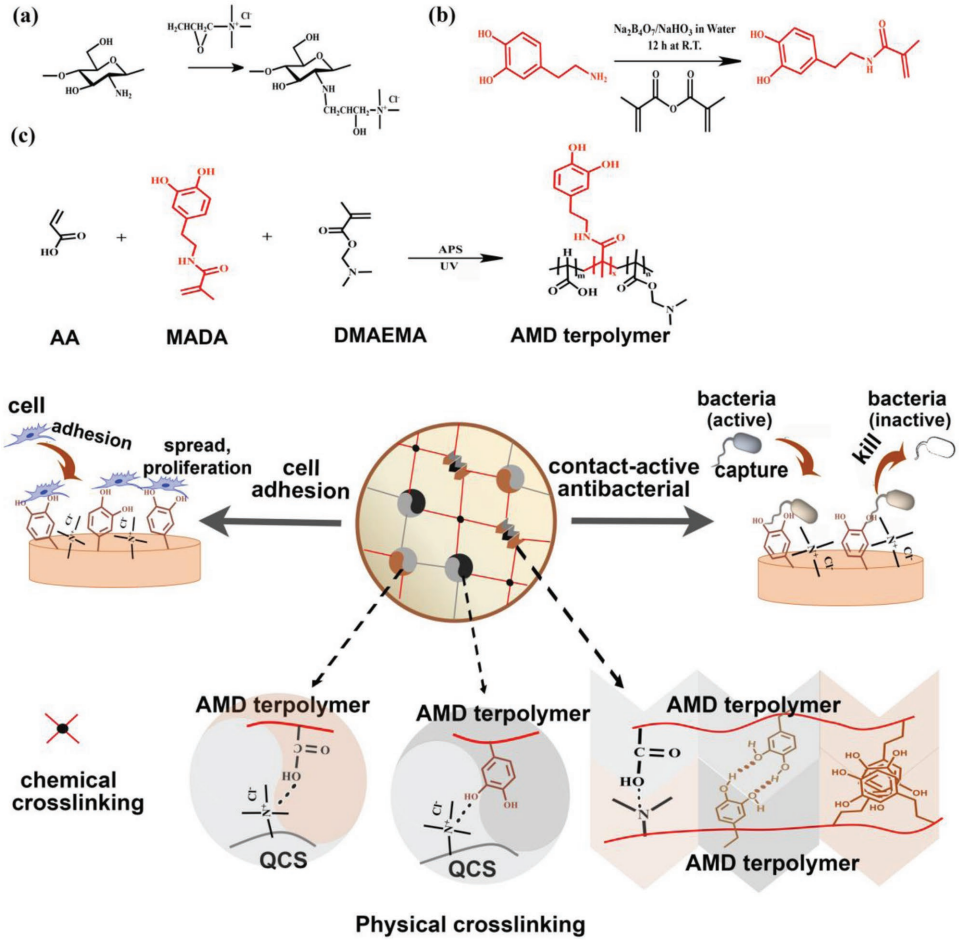

Figure 1. Design strategy of the ultra-tough, recoverable, cell-affinitive, and contact-antibacterial AMD-QCS hydrogel. a) The chemical structure of QCS and b) MADA, and c) the structure and function of the hydrogel.

MADA and QCS, and attained a value of 9168 J m^{-2}, as demonstrated by the single-edge notched test (Figure 2j). In summary, the copolymerization of MADA conferred good recoverability on the hydrogel. The interpenetration of QCS greatly enhanced the mechanical strength of the hydrogel. MADA and QCS synergistically improved hydrogel toughness, which was because both MADA and QCS introduced a high density of noncovalent bonds by electrostatic association.

2.2. The Microstructure of the Hydrogels

The hydrogel exhibited a uniform microstructure after freeze-dried, which was tuned by the addition of MADA and QCS. The freeze-dried AD hydrogel was loose with large pores (Figure S5a, Supporting Information). Compared with the freeze-dried AD hydrogel, the freeze-dried AMD hydrogel had a dense and homogeneous microstructure (Figure S5b, Supporting Information). After QCS incorporation, the network of the freeze-dried AD-QCS hydrogel and freeze-dried AMD-QCS hydrogel become more compact (Figure S5c,d, Supporting Information). The dense microstructure of the freeze-dried AMD-QCS hydrogel was attributed to two factors. First, the copolymerization of MADA introduced more catechol groups into the polymer backbones, leading to increase the physical interaction in the hydrogel network and decrease pore size of hydrogel for that the water molecules distributed homogeneously. Second, the addition of QCS formed a semi-interpenetrating network, and the positively charged groups on the molecular chain of QCS formed a strong ionic bond with the negatively charged groups on the AMD chain.

2.3. Stable Swelling Behavior

The AMD-QCS hydrogel was stable in various environments. This hydrogel did not swell and maintained a stable shape in deionized water and artificial seawater (**Figure 3**a). We also quantified the weight swelling ratio of the hydrogel in different solutions. In deionized water, the weight swelling ratio of the AMD-QCS hydrogel was only 1.0 g/g, whereas that of the PAA hydrogel was 17.0 g/g (Figure 3b). In artificial seawater, the weight swelling ratio of the AMD-QCS hydrogel remained 1.0 g/g, whereas that of the PAA hydrogel decreased to 0.5 g/g (Figure 3c). In other ionic solutions, the AMD-QCS hydrogel maintained a low equilibrium swelling ratio (Figure 3d,e).

In addition, the AMD-QCS hydrogel displayed good resistance to pH variation. The pH-responsive behavior of the hydrogels

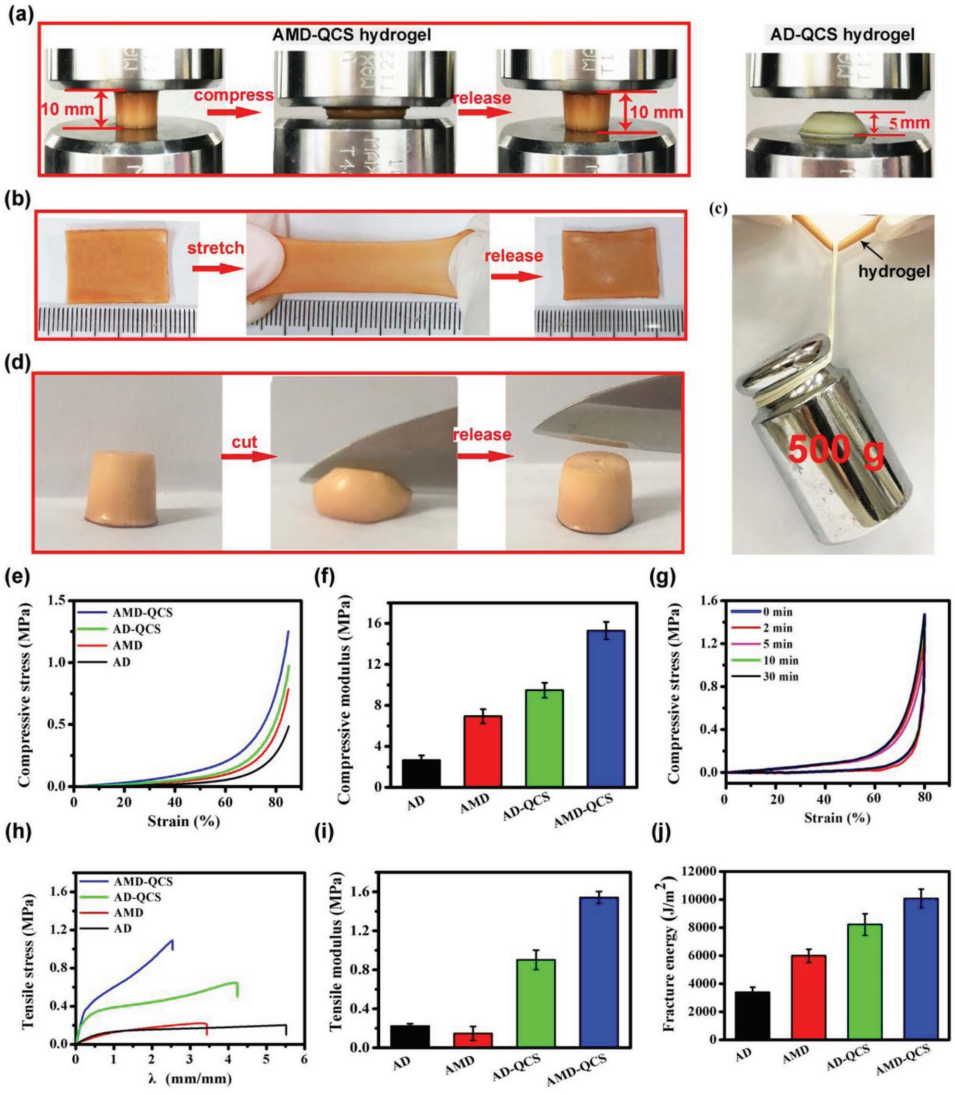

Figure 2. Mechanical properties of the hydrogels. a) Digital image showing that the AMD-QCS hydrogel has recovered its original shape (diameter of 12 mm and height of 10 mm) after it was compressed up to a strain of 85%, whereas the AD-QCS hydrogel did not. b) The AMD-QCS hydrogel has recovered its original length (width of 25 mm and thickness of 3 mm) after it was stretched to two times of its initial length. c) The AMD-QCS hydrogel (diameter of 5 mm) bore a load of 500 g. d) The AMD-QCS hydrogel (diameter of 12 mm and height of 10 mm) cuboid resisted cutting with a blade. e) Typical compression stress–strain curve. f) Compressive modulus. g) Cyclic compressive load-unload curves. h) Typical tensile stress–strain curve, i) Tensile strength, and j) Fracture energy.

was characterized by the swelling ratio versus the pH (Figure 3f). The curves of the hydrogels were U-shaped. The AMD-QCS hydrogel did not swell in the pH range of 3–12, which was much wider than that of the AD hydrogel (pH range of 5–10). Even at extremely high (pH = 13) and low (pH = 2) pH levels, the swelling ratio of the AMD-QCS hydrogels was the lowest among all the groups. In summary, these results indicated that the AMD-QCS hydrogel had a low swelling ratio in various ion solutions, which surpassed previously reported polyelectrolyte hydrogels.[16]

2.4. In Vitro Epidermal Growth Factor (EGF) Release

The AMD-QCS hydrogel displayed sustained EGF release up to 21 days (Figure S6, Supporting Information). During the initial 14 days, the amount of EGF released from the AD-QCS and AMD-QCS hydrogels was 67.1% and 52.3%, respectively. These results indicated that the EGF release rate was reduced after the copolymerization of MADA, which was mainly attributed to the interaction of the catechol groups of MADA with the proteins through Schiff's base reactions or Michael-type addition.[17]

2.5. In Vitro Antibacterial Test

The AMD-QCS hydrogel displayed strong antibacterial activities because of the synergistic effects of MADA, QCS, and DMAEMA. Antibacterial activity of the hydrogel was evaluated against *Staphylococcus epidermidis* (Gram-positive bacterium)

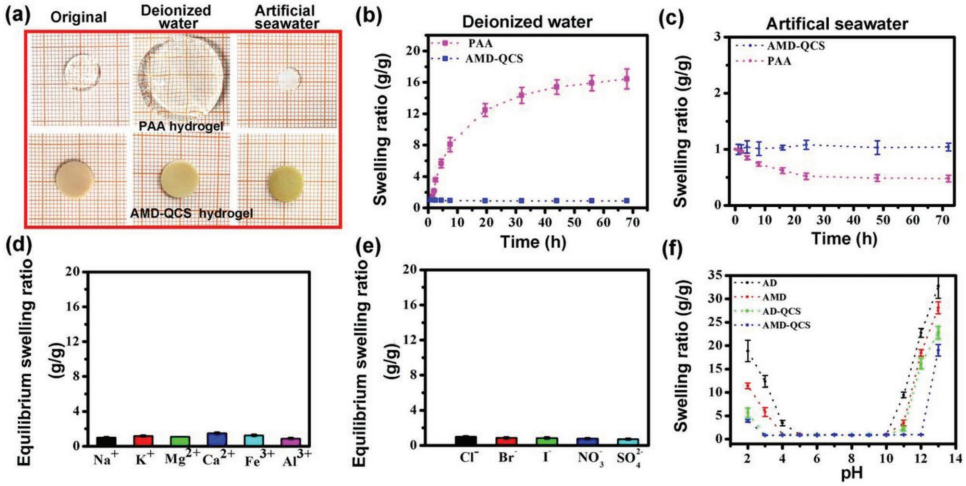

Figure 3. Swelling ability of the hydrogels. a) Images of PAA and AMD-QCS hydrogels (diameter of 10 mm and thickness of 3 mm) swollen in different environments after 60 h. b) The swelling behavior in deionized water, and c) artificial seawater. d) The swelling ratio of AMD-QCS in the solution with different cations and e) anions. f) The swelling ratios of various hydrogels in the solutions with different pH values after 60 h.

and *Escherichia coli* (Gram-negative bacterium). Images of bacterial suspensions that were co-cultured with hydrogels are presented in **Figure 4**a. Compared with the blank group, the suspensions of the AD hydrogel were clear, because the cationic DMAEMA has antibacterial activity.[18] QCS addition (AD-QCS) further promoted the antibacterial effects. Interestingly, after MADA was copolymerized (AMD-QCS), the antibacterial effects were enhanced further. The AMD-QCS hydrogel suspensions were clearest, indicating almost complete killing of bacteria.

Quantitative analysis indicated that the bactericidal ratios of *S. epidermidis* on the AD and the AMD hydrogels were 23% and 44%, respectively (Figure 4b). Interestingly, the AD-QCS and the AMD-QCS hydrogels had higher bactericidal ratios (70% and 87%, respectively) than that of their counterparts without MADA. The bactericidal ratios of the hydrogel for *E. coli* exhibited a similar trend (Figure 4b). In summary, the AMD-QCS hydrogel effectively and significantly inhibited both a Gram-negative and Gram-positive bacterium. The wide-spectrum bactericidal ability of QCS and DMAEMA endowed good antibacterial ability to the hydrogel, and this antibacterial activity was further enhanced by MADA copolymerization.

2.6. In Vivo Antibacterial Activity

The antibacterial activity of the AMD-QCS hydrogel was investigated in vivo by implanting the hydrogel subcutaneously in the presence of *E. coli*. Seven days' postsurgery, the wounds of the surgical sites were photographed (Figure 4c,d). The wounds of the control group still had a scar with pustule, whereas the wounds treated with the hydrogel were nearly closed. The surgical sites were subsequently cut open to expose any infection and the inflammatory reactions under the skin. The control group was filled with purulence (Figure 4e,f), whereas the tissue around the hydrogel did not exhibit infection. The tissue surrounding the defects was excised and stained using hematoxylin and eosin (H&E) to assess the infection. In the control group, there were a large number of multinucleated giant cells and oedema tissue, indicating severe inflammation reactions in the surrounding tissues (Figure 4g). In the AMD-QCS hydrogel-treated group, the infection was significantly reduced and there were only several minor infection cases, and the skin tissue surrounding the hydrogel was well maintained (Figure 4g). The results indicated that the AMD-QCS hydrogel can effectively kill bacterial in vivo and can thus be used for treating a wound that has succumbed to infection.

2.7. In Vitro Cell Culture

The AMD-QCS hydrogel possessed good cell affinity and favored cell adhesion and attachment. Fibroblasts, the typical cell type primarily responsible for wound repair, were cultured on various hydrogels. Confocal laser scanning microscopy micrographs revealed that the fibroblasts on the AD hydrogel retained a globular shape (**Figure 5**a), indicating that the polyampholyte AD hydrogel did not favor cell adhesion or spreading, which is consistent with previous reports.[19] After QCS incorporation, the fibroblasts had spread more, which indicated that the introduction of biopolymer QCS enhanced the cell affinity of the hydrogel (Figure 5b). By contrast, the fibroblasts adhered well on the MADA-incorporated hydrogels, both the AMD hydrogel (Figure 5c) and the AMD-QCS hydrogel (Figure 5d). These results indicated that the copolymerization of MADA into hydrogels significantly enhanced cell adhesion and attachment. The MTT assay further quantitatively evaluated cell proliferation on hydrogels after 3 and 5 days of culture (Figure 5e). After 3 days of culture, the number of cells on the AMD and AMD-QCS hydrogels was higher than that on the AD and AD-QCS hydrogels, indicating that MADA facilitates cell adhesion at the initial stage. After 5 days of culture, fibroblasts proliferated on all hydrogels, and the number of cells on the AMD-QCS hydrogel was the highest among all the groups. These results indicated that MADA played a critical role in promoting cellular adhesion and proliferation on the hydrogels.[20]

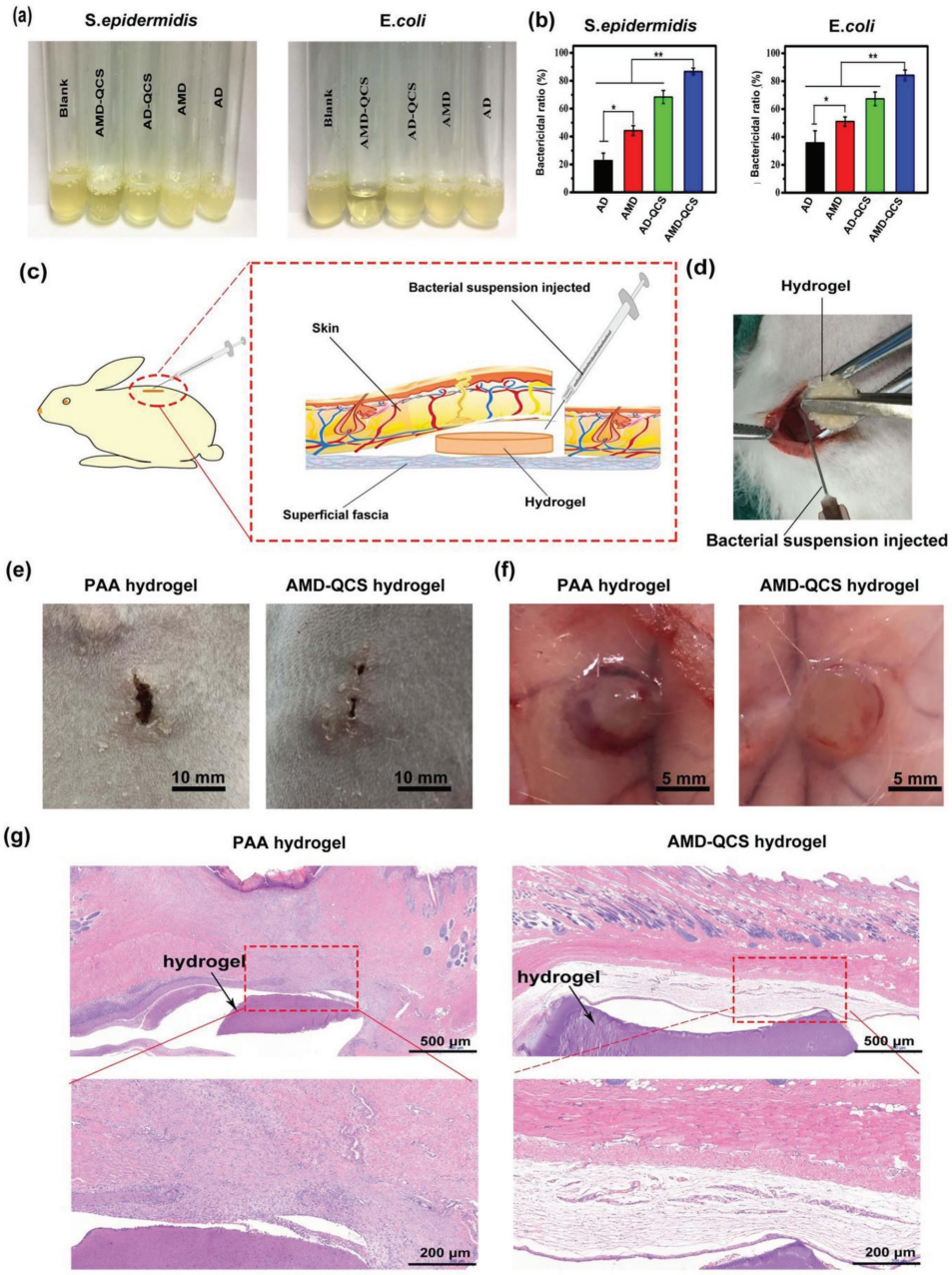

Figure 4. Antibacterial activity of the AMD-QCS hydrogel. a) *S. epidermidis* and *E. coli* suspensions that were cultured with different specimens for 24 h. b) Optical density measurement of growth of *S. epidermidis* and *E. coli* that were cultured with different specimens for 24 h. c) Schematics and d) images of the AMD-QCS hydrogel (diameter of 10 mm and thickness of 3 mm) serving as antibacterial biomaterial on the wound pockets of a rabbit. e) Images of implant sites. f) The harvested hydrogel in the wound pockets after 7 days. g) Histological examination of the tissues surrounding the hydrogel.

2.8. In Vivo Wound Healing

The AMD-QCS hydrogel can be applied to accelerate wound healing. The full-skin defect repairing experiments confirmed the enhanced wound-healing ability of the hydrogel. To further promote tissue regeneration, EGF (30 μg/sample) was loaded on the hydrogel. The images of the wound-healing process showed that the defect areas were closed in all groups after 21 days of healing (**Figure 6**a). The MADA copolymerized hydrogel (the AMD-QCS hydrogel) displayed better healing than the blank group and the group without MADA (the AD-QCS hydrogel). It was observed that hair covered the healing defects of the AMD-QCS hydrogel after 21 days of implantation, and the EGF-loaded hydrogel displayed the best healing performance. Quantitative evaluation of the wound healing of the defect area indicated that the difference in the healing ratio was prominent at the initial stage. The AMD-QCS hydrogel had a higher healing ratio of 36.5% than that of the blank group (22.5%) and the AD-QCS hydrogel (14.5%) after 7 days of treatment. EGF loading further accelerated wound healing, with the highest healing ratio of 50.2% (Figure 6b).

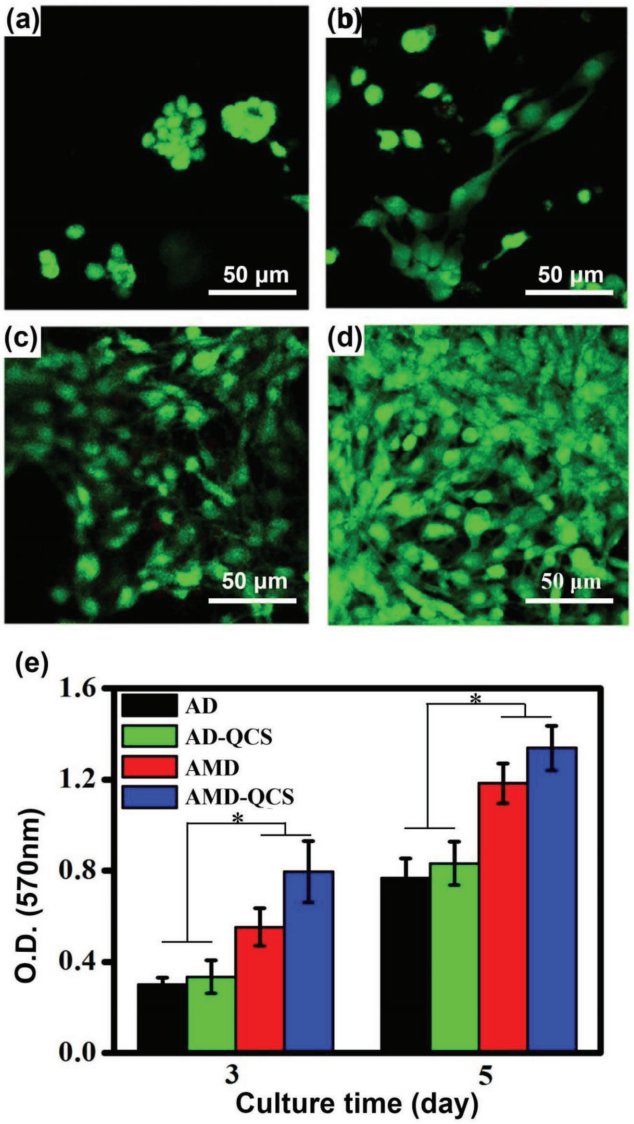

Figure 5. Cytocompatibility of the various hydrogels. Confocal laser scanning microscopy images of fibroblasts adhered on the a) AD hydrogel, b) AD-QCS hydrogel, c) AMD hydrogel, and d) AMD-QCS hydrogel after 3 days (green fluorescence represented the Calcein-AM stained living cells). e) Cell proliferation on hydrogels after 3 and 5 days of culture.

Histological analysis was used to assess the quality of the regenerated skin tissue in the defects treated with hydrogel. All groups were covered with a complete layer of epidermis after 21 days (Figure 6c). The regenerated tissue is marked by arrows in Figure 6d 1–4. The blank group displayed the largest area of immature tissue. The MADA copolymerized group (AMD-QCS) resulted in good tissue regeneration, and the area of immature tissue was reduced, with the presence of a large number of blood vessels and hair follicles. EGF-load samples displayed the best regeneration ability and only a small portion of immature tissue was observed. Most of the defect area was filled with regenerated mature skin tissue with well-arranged collagen fibers, blood vessels, and hair follicles.

The magnified sections further revealed the quality of the newly regenerated tissue (Figure 6d 5–8). In the blank group, there was much granulation tissue (marked by black arrows), which revealed that tissue was immature. In the defect treated with the AD-QCS hydrogel, more granulation tissue was replaced by collagen fibers. After treatment with the AMD-QCS hydrogel, the healing was accelerated, and the mature tissue occupied the defect area with hair follicles. In summary, the hydrogel was beneficial for wound healing and skin tissue repair. MADA copolymerization improved the effect on wound healing because of its affinity for cells/tissue and growth factors.

3. Discussion

The results of the present study demonstrated that, unlike previously reported antibacterial hydrogels, the AMD-QCS hydrogel exhibited excellent contact-active antibacterial activities. In this hydrogel, two components were used to realize wide-spectrum antibacterial activity. First, DMAEMA in the backbone has bacteriostatic antimicrobial activity against a range of Gram-negative and Gram-positive bacteria.[18] Second, QCS is another widely employed potent antibacterial biopolymer.[21] Therefore, the hydrogel exhibited an excellent antibacterial performance both in vitro and in vivo. Interestingly, the current study revealed that copolymerization of MADA led to a more effective antibacterial behavior of the hydrogel, because the large number of catechol groups of MADA improved the antibacterial contact ability of DMAEMA and QCS. These long-term and efficient antibacterial properties suggest that the hydrogel will have a wide application in implantation, particularly for repairing skin and to improve wound healing, in which prevention of inflammation of the defect is crucial.

Different from recently reported polyampholyte hydrogels that were generally cell repellent,[19] the AMD-QCS hydrogel exhibited high cell and tissue affinities because of the reactive catechol groups of MADA, and therefore this hydrogel was effective in wound healing. Traditional polyampholyte hydrogels are synthesized using organic monomers, which have no active groups to favor cell attachment or tissue integrity. For example, Gong and co-workers[22] described a series of physical hydrogels composed of polyampholytes with high toughness and viscoelasticity. However, these polyampholyte hydrogels are analogous to zwitterion polymers, which are inadequate for cell adhesion and proliferation. In the present hydrogel, MADA was copolymerized into the hydrogel to endow it with cell and tissue adhesive properties. Catechol groups of MADA can form both covalent binding through Michael addition or Schiff's base reactions and noncovalent binding via hydrogen bonding and π–π stacking with cell or tissue surfaces. Therefore, this hydrogel could be used for wound healing and tissue regeneration.

The AMD-QCS hydrogel have both contact-active antibacterial ability and cytocompatibility, which is based on the synergistic effects of MADA, QCS, and DMAEMA. The MADA enhances the bacterial capture ability of the hydrogel. Thus, the reactive catechol groups of MADA endow the hydrogel with contact intensified bactericidal activity, because they increase

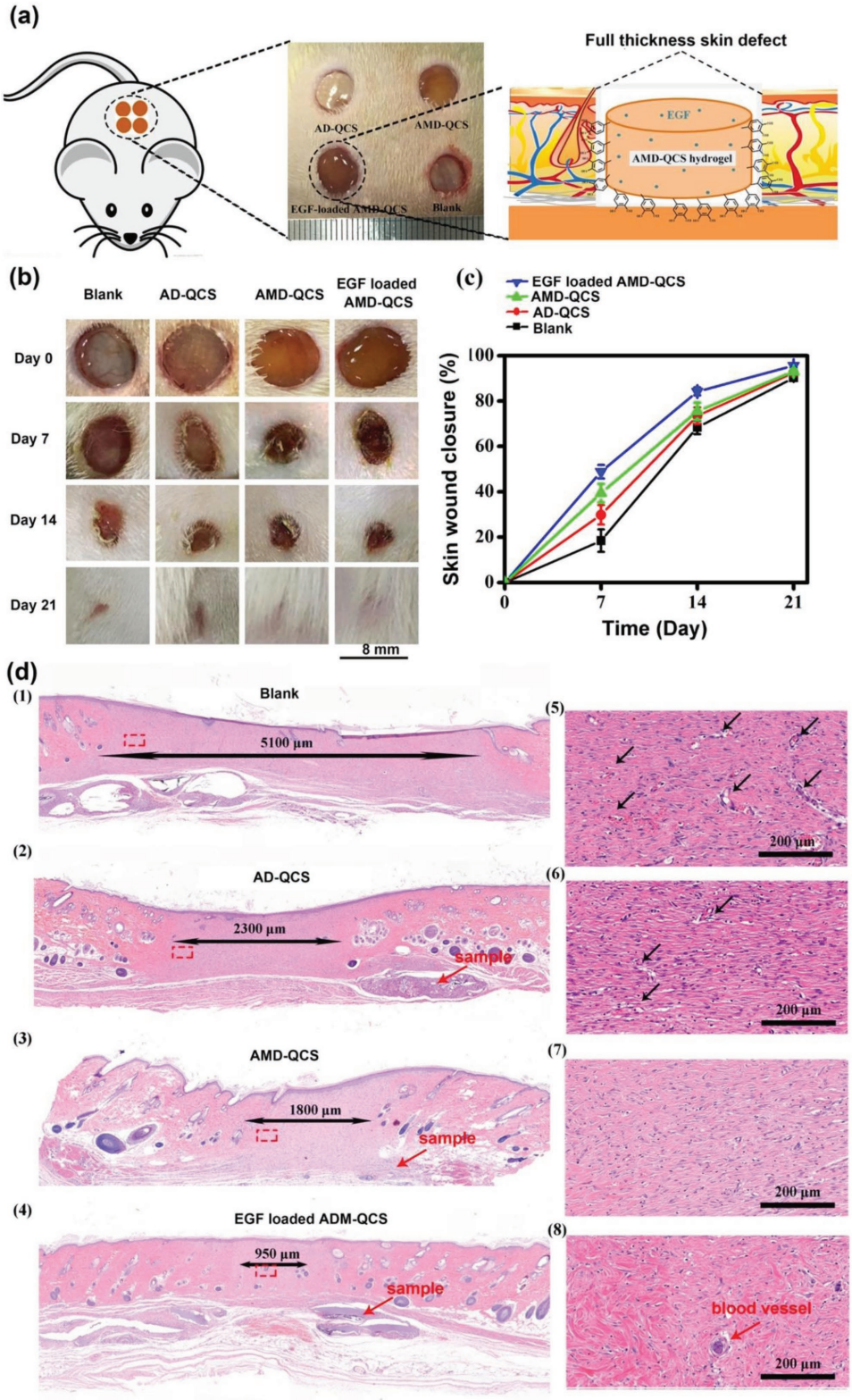

Figure 6. a) Schematics of hydrogel implantation for wound repair. b) Representative images of the gross appearance of defects treated with AD-QCS, AMD-QCS, or EGF-loaded AMD/QCS (diameter of 8 mm and thickness of 2 mm) after different period of implantation. c) Percentage of wound closure after different periods. d) HE staining of wound sections after 21 days of treatment. The right columns are the magnified image of the area marked by the rectangles in the left column (black arrows represent granulation tissue).

the exposure of bacterium cells to the positively charged groups of the hydrogel and strengthen the bactericidal effect. To further prove this point, the adhesion of bacteria on the AMD-QCS hydrogel and AD-QCS hydrogel was assessed by culturing *E. coli* and *S. epidermidis* suspension with the hydrogels. As shown in Figure S7 in the Supporting Information, AMD-QCS hydrogel have more adhered bacteria than AD-QCS hydrogel for both *E. coli* and *S. epidermidis,* which indicated that the AMD-QCS can better capture bacteria with the presence of MADA. QCS and DMAEMA are the critical components to endow the hydrogel with antibacterial activity. The antibacterial behavior is closely related to the charge density on the cell wall of bacterial.[23] The Gram-positive bacterium cell wall is composed of peptidoglycan and teichoic-acid.[24] The permeability of bacterium cell wall is changed when they contact with the hydrogel because polycationic QCS and DMAEMA have strong electrostatic attraction with polyanionic teichoic-acid. Consequently, the bacterial are disrupted and killed by the hydrogel.[25] The mechanism of killing Gram-negative bacterial is different from that of Gram-positive bacterium. QCS and DMAEMA can destroy the stability of bacterium structure and cause cell death by chelating the divalent cations from the outer membrane of Gram-negative bacteria.[26] On the other hand, the cytocompatibility of AMD-QCS hydrogel is contributed by the catechol groups of MADA and the inherent biocompatibility of QCS. It has been proved that the catechol groups of dopamine can improve the cell adhesion and endow the materials with good cell/tissue affinity.[27] QCS is the derivative of CS that is well proved to be biocompatible for cells. Furthermore, because of the different cell membrane structure between cells and bacterial the QCS cannot penetrate the lipid bilayer of cell, and therefore the QCS have low cytotoxicity.[28]

Our AMD-QCS polyampholyte hydrogels also displayed good recoverability and toughness because of the copolymerized MADA in the backbone. Of note, previously reported polyampholyte hydrogels were generally stiff, but lacked recoverability,[9a,29] because they were mainly composed of positively and negatively charged monomers. Therefore, there were strong electrostatic interactions between the charge groups, thereby restricting movement of the chain. In our study, MADA was copolymerized into the chain, which led to good recoverability because of two reasons. First, MADA weakens the electrostatic interaction between the functional groups of cationic and ionic monomers. Second, MADA also introduces more reversible noncovalent interaction, including hydrogel bonding and π–π interaction, into the hydrogel networks. These reversible bonds break and reform during deformation to dissipate energy, and therefore endow the hydrogel with toughness and recoverability.

In contrast to the previously reported pH- and ionic-sensitive polyampholyte hydrogels, our AMD-QCS hydrogel was stable in various environments, including deionized water, artificial seawater, and solutions with various ions as well as over a wide range of pH values. Generally, the noncovalent bonds of a polyampholyte hydrogel will be weakened when the hydrogel is soaked in physiological or ionic solutions. Swelling drastically disrupts the network structure and reduces the mechanical properties of a hydrogel. For example, Liu et al.[30] reported a form of poly(DMAEMA-co-AA) hydrogel with a swelling ratio of 734% and strait pH values ranging. Sun et al.[31] designed a copolymer of cationic (3-(methacryloylamino) propyl-trimethylammonium chloride and anionic (p-styrenesulfonate) monomers hydrogel with a swelling volume ratio of 10 v/v. In the current study, MADA was copolymerized into the hydrogel, increasing its noncovalent bond density, thereby preventing ion and water absorption into the hydrogel. Consequently, the AMD-QCS hydrogel did not swell under various conditions.

4. Conclusion

In summary, we demonstrated a contact-active antibacterial AMD-QCS hydrogel, which realized the combination of effective antibacterial ability and excellent cell affinity. The hydrogel was inherently antimicrobial because of the two typically polycationic (QCS, DMAEMA) polymers in the network. Particularly, MADA intensified the antibacterial effect of the polycationic polymers by improving the bacterial contact with the hydrogel. Furthermore, because of the catechol groups of MADA in the terpolymer, the hydrogel facilitated cell adhesion and exhibited high tissue affinity. Therefore, this mussel-inspired hydrogel with inherent long-term and effective antibacterial ability not only can avoid many problems associated with using antibiotics, including high cost, short half-life, bacterial resistance, and burst release but also provide a new solution to balance the cell compatibility and antibacterial activity of biomaterials. In short, this study for the first time proposed a new strategy to form a contact-active antibacterial hydrogel, which is a breakthrough to overcome the shortcomings of traditional antibacterial hydrogels that are cell repellent.

The hydrogel exhibited a good mechanical performance, including high toughness and good recoverability, because of the large number of electrostatic interactions created in the network. Unlike previously reported synthetic polyelectrolyte hydrogels with high swelling ratio, the current hydrogel is a synthetic/biopolymer hybrid, and therefore exhibited a low swelling ratio in a complicated environment. In addition, the hydrogel was able to immobilize EGF and allowed its sustained release, because of the presence of catechol groups in MADA. The hydrogel was successfully applied for skin wound healing, demonstrating that this tough polyelectrolyte hydrogel can be used for skin tissue repair. Compared with previous tough or antibacterial hydrogels, this hydrogel, integrating antibacterial ability, cell affinity, and good mechanical properties, is more suitable for soft tissue repair while protecting it from infection.

5. Experimental Section

Synthesis of the AMD-QCS Hydrogel: Before hydrogel synthesis, a high-throughput study was performed to screen for a suitable mass ratio of AA to DMAEMA, which was determined as 7:3 (Details in Table S2 and Figure S1, Supporting Information).

To prepare the AMD-QCS hydrogel, QCS were dissolved in deionized water followed by the addition of DMAEMA, AA, and MADA monomer. Following mixing and degassing, the solution was copolymerized at 60 °C for 20 min in the presence of an initiator ammonium persulfate (APS) and cross-linker (PEGDA). The compositions of the different hydrogels are listed in Table S3 in the Supporting Information.

Mechanical Properties Tests: The tensile and compression tests were performed on a universal test machine (UTM, Instron 5567, USA). For tensile testing, the specimens were of 20 mm width and 2 mm thickness, with a testing gauge length of 5 mm. For compression testing, the hydrogels had a cylindrical shape (height 10 mm, diameter 5 mm). The fracture energy of the hydrogels was determined by the classical single-edge notch test on the UTM machine (Instron 5567). Details are provided in the Supporting Information.

Swelling Tests: To measure the swelling ratios, the hydrogels were swollen at 25 °C until the equilibrium state was reached in the different environments, including artificial seawater, NaOH-HCl solutions with different pH values, and different ionic solutions. The composition of the solutions is provided in the Supporting Information. The swelling ratio was determined by the following equation:

$$\text{Swelling ratio} = W_S/W_0 \quad (1)$$

W_0 was the weight of initial samples and W_S was the weight of the swollen sample.

Biocompatibility Test: NIH-3T3 fibroblasts (Stem Cell Bank, Chinese Academy of Sciences, SCSP-515) were cultured on the AD, AMD, AD-QCS, and AMD-QCS hydrogels. There were four parallel samples for each hydrogel. The procedure followed the previous study.[27] Briefly, before cell seeding, the hydrogels with diameter 8 mm and thickness 2.5 mm were first purified in phosphate-buffered saline (PBS) and sterilized with 75% ethanol for 24 h. The hydrogels were then immersed in Dulbecco minimum essential medium (DMEM) and swelled to an equilibrium state. Cells on the hydrogels were stained using Calcein AM (A017, GeneCopoeia Inc. USA), and observed using a confocal laser scanning microscope (TCSSP5, Leica, Germany). The cell growth on the hydrogels was quantified using the MTT assay. Details are described in the Supporting Information.

In Vitro Antibacterial Activity: S. epidermidis (ATCC 12228) and *E. coli* (ATCC 8739) were used to evaluate the antibacterial activity of the hydrogels. During antibacterial tests, the AD, AMD, AD-QCS, and AMD-QCS hydrogels were selected as the experimental groups. And the specimens without hydrogel were set as blank group. Four parallel specimens of each group were used for the antibacterial test. The procedure was according to the previous study.[32] Details are described in the Supporting Information.

In Vivo Antibacterial Activity: The antibacterial activity of the AMD-QCS hydrogel was evaluated in vivo in a rabbit subcutaneous model. Experiments were performed in four New Zealand rabbits (Dashuo, Chengdu, China), weighing 2–3 kg. AMD-QCS hydrogels were implanted in the subcutaneous pocket on the back of each rabbit and the AA hydrogel was also implanted as a control. All implants were sterilized using 75 wt% alcohol prior to implantation. Following implantation of the samples, the subcutaneous pocket was inoculated with an *E. coli* suspension (0.2 mL, 10^8 CFU/mL). The rabbits were housed individually and given access to food and water ad libitum. The animals were observed daily and were euthanized after one week postoperation. The sample together with each pocket was excised en bloc. Specimens were fixed in 10% formalin and embedded in paraffin blocks. Tissue sections were mounted onto slides, which were then stained using Hematoxylin and Eosin.

In Vivo Wound Healing: Different hydrogels were used to repair skin defects. Full-thickness skin wounds were created on the dorsal area of Sprague Dawley (SD) rats (Dashuo, Chengdu). The defects were treated using the following hydrogels: 1) AD-QCS hydrogel, 2) AMD-QCS hydrogel, 3) EGF-loaded AMD-QCS hydrogel (30 μg EGF/sample), 4) untreated defects were set as the blank group. Experiments were performed in four SD rats, and four parallel specimens of each type of hydrogel were implanted. The surgical procedure followed the previous study.[11] The details are described in the Supporting Information. All animal experiments were performed in accordance with protocols approved by the local ethical committee and laboratory animal administration rules of China.

Statistical Analysis: One-way analysis of variance (ANOVA) followed by Tukey multiple-comparison post hoc test was conducted to determine the significant difference between groups.

Supporting Information

Supporting Information is available from the Wiley Online Library or from the authors.

Acknowledgements

D.G. and T.X. contributed equally to this work. This work was financially supported by the National key research and development program of China (2016YFB0700800), NSFC (81671824), Fundamental Research Funds for the Central Universities (2682016CX075, 2682018QY02), Natural Science Foundation of Tianjin (18JCYBJC19500). Independent Innovation Fund of Tianjin University (2018XGP-0030), and the open fund of Tianjin Key Laboratory of Equipment Design and Manufacturing Technology.

Conflict of Interest

The authors declare no conflict of interest.

Keywords

contact-active antibacterial, mussel inspired, tough hydrogel, wound healing

Received: August 25, 2018
Revised: October 17, 2018
Published online: November 13, 2018

[1] a) M. C. Giano, Z. Ibrahim, S. H. Medina, K. A. Sarhane, J. M. Christensen, Y. Yamada, G. Brandacher, J. P. Schneider, *Nat. Commun.* **2014**, *5*, 4095; b) S. Li, S. Dong, W. Xu, S. Tu, L. Yan, C. Zhao, J. Ding, X. Chen, *Adv. Sci.* **2018**, *5*, 1700527.
[2] P. Li, Y. F. Poon, W. Li, H. Y. Zhu, S. H. Yeap, Y. Cao, X. Qi, C. Zhou, M. Lamrani, R. W. Beuerman, *Nat. Mater.* **2011**, *10*, 149.
[3] Y. Ren, X. Zhao, X. Liang, P. X. Ma, B. Guo, *Int. J. Biol. Macromol.* **2017**, *105*, 1079.
[4] a) R. O. Darouiche, *Clin. Infect. Dis.* **2001**, *33*, 1567; b) S. R. Deka, A. K. Sharma, P. Kumar, *Curr. Top. Med. Chem.* **2015**, *15*, 1179.
[5] G. Du, L. Nie, G. Gao, Y. Sun, R. Hou, H. Zhang, T. Chen, J. Fu, *ACS Appl. Mater. Interfaces* **2015**, *7*, 3003.
[6] a) C. B. Rodell, N. N. Dusaj, C. B. Highley, J. A. Burdick, *Adv. Mater.* **2016**, *28*, 8419; b) M. Mti, N. Kitamura, T. Nonoyama, S. Wada, K. Goto, X. Zhang, T. Nakajima, T. Kurokawa, Y. Takagi, K. Yasuda, *Biomaterials* **2017**, *132*, 85.
[7] N. Rauner, M. Meuris, M. Zoric, J. C. Tiller, *Nature* **2017**, *543*, 407.
[8] D. R. King, T. L. Sun, Y. Huang, T. Kurokawa, T. Nonoyama, A. J. Crosby, J. P. Gong, *Mater. Horiz.* **2015**, *2*, 584.
[9] a) A. B. Ihsan, T. L. Sun, S. Kuroda, M. A. Haque, T. Kurokawa, T. Nakajima, J. P. Gong, *J. Mater. Chem. B* **2013**, *1*, 4555; b) F. Luo, T. L. Sun, T. Nakajima, T. Kurokawa, Y. Zhao, A. B. Ihsan, H. L. Guo, X. F. Li, J. P. Gong, *Macromolecules* **2014**, *47*, 6037.
[10] J. You, S. Xie, J. Cao, H. Ge, M. Xu, L. Zhang, J. Zhou, *Macromolecules* **2016**, *49*, 1049.
[11] L. Han, X. Lu, K. Liu, K. Wang, L. Fang, L. T. Weng, H. Zhang, Y. Tang, F. Ren, C. Zhao, *ACS Nano* **2017**, *11*, 2561.
[12] C. Shao, M. Wang, L. Meng, H. Chang, B. Wang, F. Xu, J. Yang, P. Wan, *Chem. Mater.* **2018**, *30*, 3110.
[13] D. E. Fullenkamp, J. G. Rivera, Y. K. Gong, K. H. Lau, L. He, R. Varshney, P. B. Messersmith, *Biomaterials* **2012**, *33*, 3783.
[14] L. García-Fernández, J. Cui, C. Serrano, Z. Shafiq, R. A. Gropeanu, V. S. Miguel, J. I. Ramos, M. Wang, G. K. Auernhammer, S. Ritz,

A. A. Golriz, R. Berger, M. Wagner, A. del Campo, *Adv. Mater.* **2013**, *25*, 529.
[15] T. S. Sileika, H.-D. Kim, P. Maniak, P. B. Messersmith, *ACS Appl. Mater. Interfaces* **2011**, *3*, 4602.
[16] J. Lam, E. C. Clark, E. L. S. Fong, E. J. Lee, S. Lu, Y. Tabata, A. G. Mikos, *Biomaterials* **2016**, *83*, 332.
[17] Y. Liu, K. Ai, L. Lu, *Chem. Rev.* **2014**, *114*, 5057.
[18] H. Murata, R. R. Koepsel, K. Matyjaszewski, A. J. Russell, *Biomaterials* **2007**, *28*, 4870.
[19] T. L. Sun, T. Kurokawa, S. Kuroda, A. B. Ihsan, T. Akasaki, K. Sato, M. A. Haque, T. Nakajima, J. P. Gong, *Nat. Mater.* **2013**, *12*, 932.
[20] D. Hafner, L. Ziegler, M. Ichwan, T. Zhang, M. Schneider, M. Schiffmann, C. Thomas, K. Hinrichs, R. Jordan, I. Amin, *Adv. Mater.* **2016**, *28*, 1489.
[21] R. R. Mohamed, M. H. Elella, M. W. Sabaa, *Int. J. Biol. Macromol.* **2017**, *98*, 302.
[22] C. K. Roy, H. L. Guo, T. L. Sun, A. B. Ihsan, T. Kurokawa, M. Takahata, T. Nonoyama, T. Nakajima, J. P. Gong, *Adv. Mater.* **2015**, *27*, 7344.
[23] M. Kong, X. G. Chen, K. Xing, H. J. Park, *Int. J. Food Microbiol.* **2010**, *144*, 51.
[24] D. H. Young, H. J. P. P. Kauss, *Plant Physiol.* **1983**, *73*, 698.
[25] E. I. Rabea, M. E.-T. Badawy, C. V. Stevens, G. Smagghe, W. J. B. Steurbaut, *Biomacromolecules* **2003**, *4*, 1457.
[26] M. Ignatova, K. Starbova, N. Markova, N. Manolova, I. Rashkov, *Carbohydr. Res.* **2006**, *341*, 2098.
[27] L. Han, X. Lu, M. Wang, D. Gan, W. Deng, K. Wang, L. Fang, K. Liu, C. W. Chan, Y. J. S. Tang, *Small* **2017**, *13*, 1601916.
[28] a) Y. Yang, H. Ao, Y. Wang, W. Lin, S. Yang, S. Zhang, Z. Yu, T. T. Tang, *Bone Res.* **2016**, *4*, 16027; b) Y. Yang, S. B. Yang, Y. Wang, Z. F. Yu, H. Y. Ao, H. B. Zhang, L. Qin, O. Guillaume, D. Eglin, R. G. Richards, T. T. Tang, *Acta Biomaterialia.* **2016**, *46*, 112.
[29] K. Cui, T. L. Sun, T. Kurokawa, T. Nakajima, T. Nonoyama, L. Chen, J. P. Gong, *Soft Matter* **2016**, *12*, 8833.
[30] Y. Liu, C. Wang, S. Chen, *RSC Adv.* **2015**, *5*, 30514.
[31] T. L. Sun, F. Luo, T. Kurokawa, S. N. Karobi, T. Nakajima, J. P. Gong, *Soft Matter* **2015**, *11*, 9355.
[32] C. Xie, X. Lu, K. Wang, *Part. Part. Syst. Charact.* **2015**, *32*, 630.